ACS APPLIED MATERIALS & INTERFACES

Research Article

www.acsami.org

Bifunctional Sensing Characteristics of Chemical Vapor Deposition Synthesized Atomic-Layered MoS_2

Byungjin Cho,*[,†] Ah Ra Kim,[†] Youngjin Park,[†] Jongwon Yoon,[‡] Young-Joo Lee,[†] Sangchul Lee,[‡,§] Tae Jin Yoo,[‡] Chang Goo Kang,[‡,∥] Byoung Hun Lee,[‡] Heung Cho Ko,[‡] Dong-Ho Kim,*[,†] and Myung Gwan Hahm*[,†]

[†]Advanced Functional Thin Films Department, Surface Technology Division, Korea Institute of Materials Science (KIMS), 797 Changwondaero, Sungsan-gu, Changwon, Gyeongnam 642-831, Republic of Korea

[‡]School of Materials Science and Engineering, Gwangju Institute of Science and Technology (GIST), 123 Cheomdangwagiro, Buk-gu, Gwangju 500-712, Republic of Korea

Supporting Information

ABSTRACT: Two-dimensional (2D) molybdenum disulfide (MoS_2) atomic layers have a strong potential to be adopted for 2D electronic components due to extraordinary and novel properties not available in their bulk foams. Unique properties of the MoS_2, including quasi-2D crystallinity, ultrahigh surface-to-volume, and a high absorption coefficient, have enabled high-performance sensor applications. However, implementation of only a single-functional sensor presents a limitation for various advanced multifunctional sensor applications within a single device. Here, we demonstrate the charge-transfer-based sensitive (detection of 120 ppb of NO_2) and selective gas-sensing capability of the chemical vapor deposition synthesized MoS_2 and good photosensing characteristics, including moderate photoresponsivity (~71 mA/W), reliable photoresponse, and rapid photoswitching (<500 ms). A bifunctional sensor within a single MoS_2 device to detect photons and gas molecules in sequence is finally demonstrated, paving a way toward a versatile sensing platform for a futuristic multifunctional sensor.

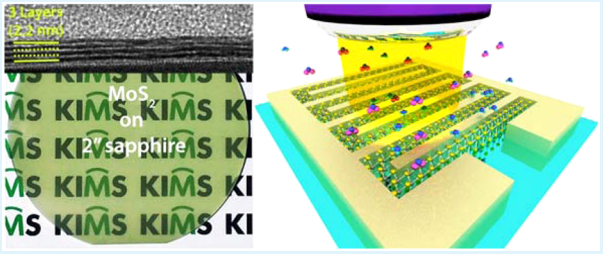

KEYWORDS: *MoS_2, CVD synthesis, gas sensor, photodetector, bifunctional sensor*

INTRODUCTION

Atomic-scaled low dimensional (one- or two-dimensional) nanomaterials have been attracting much interest as a strong candidate for diverse electronic and optoelectronic components.[1−8] Recently, a variety of two-dimensional (2D) transition-metal dichalcogenides (TMDs) could enable superior detection capabilities of physical or chemical parameters due to their unique physical properties, including high surface-to-volume ratio, sizable band gaps, semiconducting property, and high absorption coefficient. In particular, many researchers have struggled to show the possibility of realizing high-performance gas molecule detection[9−12] and photodetection[5,13,14] using the 2D TMD materials. On the other hand, most of the relevant studies have primarily focused on potential single function sensor applications based on mechanically exfoliated MoS_2 nanoflakes. Even though such top-down synthesis methods have resulted in high-quality crystalline structure, there are many unavoidable limitations like randomly distributed, small scaled, and thickness-uncontrollable flakes, which would not be suitable for use in realistic electronic devices and other advanced uses. This technical barrier has spurred interest in identifying an effective solution for the large-scale synthesis of MoS_2.[15−20] Furthermore, in the previous studies of gas sensors[9,10] or photodetectors[13,14,21] utilizing the 2D nanomaterials, single function sensing characteristics have been mostly investigated. In this paper, we report on the physical properties of chemical vapor deposition (CVD) synthesized MoS_2 film on a wafer scale and its bifunctional sensing characteristics. First of all, it is demonstrated that the MoS_2-based gas sensor shows an extremely low, sub-ppm detection level, high selectivity, and stable cycling behavior. Second, the MoS_2 photosensor provides reasonable photoresponsivity (~71 mA/W), reliable photoresponse, and rapid photoswitching (<500 ms). Finally, we have investigated the bifunctional sensing characteristics of the MoS_2-based devices to detect both gas molecules and a light source in sequence. These multifunctional sensing characteristics of the atomic-layered MoS_2 would also make attractive other 2D TMDs for futuristic sensor technologies.

EXPERIMENAL SECTION

CVD Synthesis of MoS_2 Nanofilms. MoS_2 nanofilms were synthesized using a chemical vapor deposition (CVD) system (Teraleader Co., Ltd.). First, C-plane sapphire substrate was prepared using a typical cleaning process (sonication in acetone, isopropyl

Received: December 4, 2014
Accepted: January 9, 2015
Published: January 9, 2015

DOI: 10.1021/am508535x
ACS Appl. Mater. Interfaces 2015, 7, 2952−2959

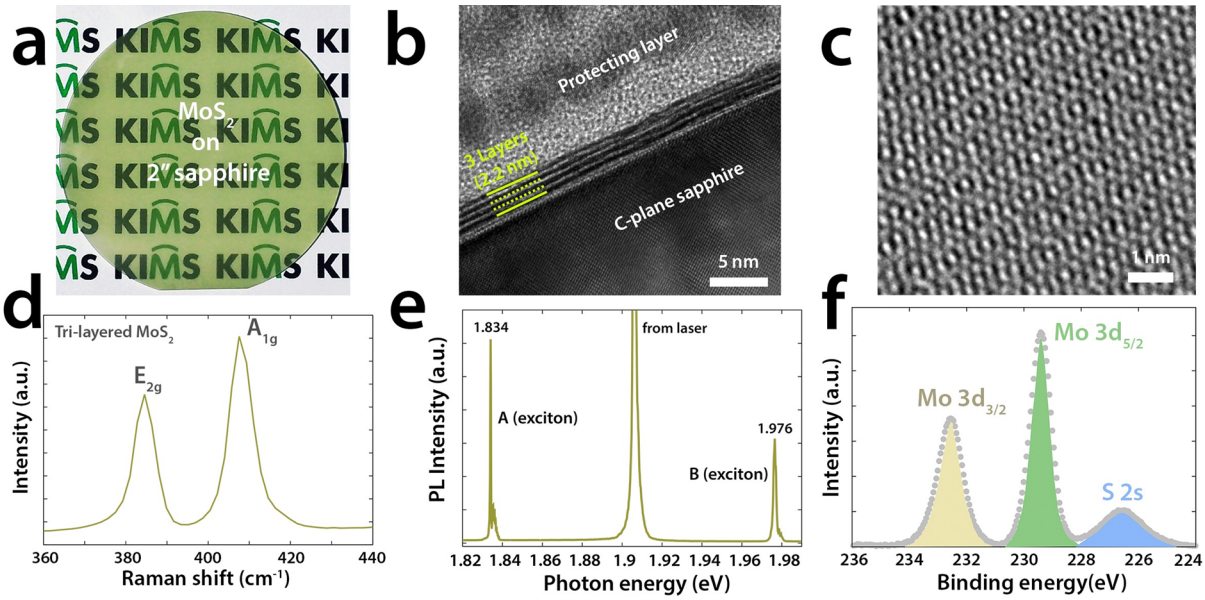

Figure 1. (a) Optical image showing the as-synthesized MoS_2 film on 2-in. sapphire substrate. The as-synthesized MoS_2 film was semitransparent. (b) Cross-sectional TEM images of the MoS_2 film. The synthesized MoS_2 films consist of trilayered MoS_2. (c) Planar TEM image showing a Moiré pattern found in overlapping misoriented layers of MoS_2 (d) Raman spectrum of trilayered MoS_2. The peak position difference (Δ) between E_{2g} and A_{1g} was approximately 23, indicating trilayered MoS_2. (e) PL spectrum of the MoS_2 film excited by the 314 nm wavelength laser line. Two major emission peaks featured at 1.834 eV (A exciton) and 1.976 eV (B exciton) are associated with the direct band gap transition of few-layered MoS_2 (f) XPS spectrum of the synthesized MoS_2 with a doublet of Mo $3d_{5/2}$ (229.4 eV) and Mo $3d_{3/2}$ (232.5 eV) and S 2s (226.6 eV).

alcohol, and deionized water for 10 min each). MoO_3 films (5 nm) were deposited on the clean substrates using a thermal evaporator. The predeposited MoO_3 samples were placed at the center of the furnace, and sulfur powder was loaded on an independently temperature controllable flange heater located near the inlet of the furnace. The furnace and flange heater were heated to ~900 and ~180 °C, respectively, for 1 h. The process was maintained for another hour under the flow of an Ar/H_2 mixture gas at a chamber pressure of 760 Torr. The MoO_3 film was converted into a MoS_2 nanofilm by a two-step reaction (the reduction of MoO_3 by hydrogen gas, followed by sulfurization of the reduced MoO_3 with sublimated sulfur gases). Finally, the furnace was rapidly cooled down to room temperature by opening the chamber box as soon as the synthesis process ended.

Characterization of the CVD-Synthesized MoS_2 Nanofilm. A focused ion beam instrument was used to prepare cross-sectional MoS_2 transmission electron microscopy (TEM) images. Planar TEM images were obtained from the MoS_2 placed on a C/Cu TEM grid. The TEM specimens were examined using a Cs-corrected TEM (JEM-ARM200F, JEOL) equipped with an energy-dispersive X-ray spectrometry detector (Quantax 400, Bruker). Raman and PL spectra were obtained using a 514 and 325 nm laser source of a confocal Raman microscopy system (LabRAM HR, Horiba Jobin Yvon SAS). Elemental composition analysis was performed using an X-ray photoelectron spectroscope (XPS) (AXIS-NOVA, Kratos Inc.) with focused monochromatized Al Kα (1486.6 eV) radiation.

Fabrication of the MoS_2 Sensing Device. C-plane sapphire was cleaned using a typical cleaning process. A MoO_3 film of ~5 nm was patterned with an active shadow mask utilizing a thermal evaporator. The patterned MoO_3 film was converted into a MoS_2 nanofilm by the CVD process. The as-grown MoS_2 on C-plane sapphire was used for gas-sensing measurements. For the photosensing and the bifunctional sensing measurement, MoS_2 transferred onto a SiO_2/p^+ Si substrate was used [transfer method is as follows: spin-coating of poly(methyl methacrylate) (PMMA) as a supporting layer on an as-grown MoS_2/sapphire Si substrate, etching of sapphire using 3 M NaOH solution, fishing out of PMMA-supported MoS_2 onto a new SiO_2/p^+ Si substrate, removal of PMMA by acetone, and finally drying of the MoS_2 film by N_2 blowing]. Using a shadow mask with an interdigitated electrode array structure with a width of 400 μm and a gap of 100 μm, a Au/Cr film (50/3 nm) for the electrodes was deposited on the MoS_2 nanofilm using the thermal evaporator.

Gas-Sensing Measurement. The gas-sensing test was conducted by exposing the MoS_2 devices (as-grown MoS_2 on C-plane sapphire substrate) to the analyte gas diluted with ultrahigh purity (99.999%) N_2 gas for 1 min. The concentrations of the analyte gases were adjusted by the flow rate ratio of both gases (N_2 and analyte gas). Using a Keithley 2401 source meter, the sensing signal of the MoS_2 devices was monitored by the resistance change at a voltage of 5 V.

Photosensing Measurement. The photonic sensing properties of the MoS_2 devices (transferred MoS_2 on the SiO_2/p^+ Si substrate) were characterized using a semiconductor parameter analyzer (Keithley 4200) in the visible range. Light-emitting diodes (wavelengths 625, 530, and 470 nm) were used as the light sources; their intensities were modulated from 0.2 to 4 mW/cm^2 using a neutral density filter. The spot size of the light source passing through the microscope lens was approximately 1 cm^2, which fully covered the active area of the MoS_2 device. The transient current responses were measured under various voltages (2−5 V) and light intensities (0.2−4 mW/cm^2). All measurements were performed in ambient air.

Bifunctional Sensing Measurement. The gas sensitivity of the MoS_2 device (transferred MoS_2 on the SiO_2/p^+ Si substrate) under illumination was verified in the same chamber used for the gas-sensing measurement. After the light source (power of 5 mW and wavelength of 650 nm) was turned on in the closed chamber, the MoS_2 devices were exposed to the analyte gas (100 ppm of NO_2 or NH_3 gas) for 1 min at the same time. All in situ sensing measurements for the simultaneous detection of photo- and gas-sensing were performed at room temperature (rt).

RESULTS AND DISCUSSION

Most synthesis approaches involve direct/indirect sulfurization of Mo-containing thin films for the atomic-layered MoS_2. The precursor is a key factor in the synthesis of MoS_2, and most studies have adopted one of three precursors: molybdenum thin film,[22] molybdenum trioxide (MoO_3),[23] and ammonium thiomolybdate.[24] In particular, we selected the second precursor as a source of transition metal among them.

DOI: 10.1021/am508535x
ACS Appl. Mater. Interfaces 2015, 7, 2952−2959

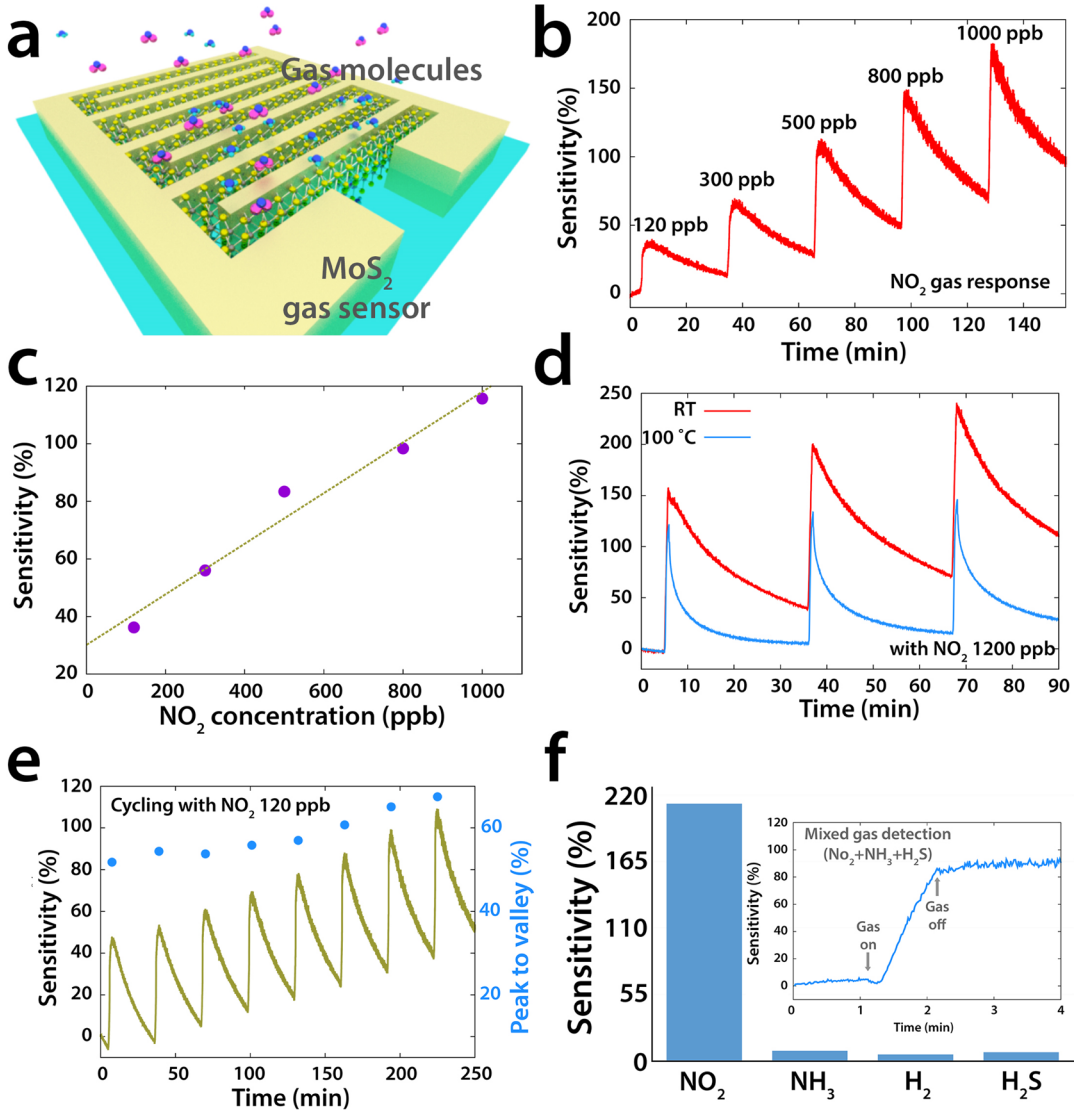

Figure 2. (a) 3D schematic image of the MoS_2 gas sensor device under gas molecules. (b) Transient NO_2 gas response of the MoS_2 device from 120 to 1000 ppb at rt. (c) Sensitivity change data of MoS_2 device upon NO_2 concentration, which was extracted from part b. The fitted line follows the linear relationship between sensitivity and concentration, which is derived from Langmuir's isotherm model. (d) NO_2 gas response behavior at 1200 ppb concentration strongly depending on operating temperature. The thermal annealing under the test enhanced recovery rate (blue line). (e) Cycling performance of NO_2 gas response at 120 ppb level. (f) Sensitivity comparison for each different gas molecule (NO_2, NH_3, H_2, and H_2S). The results shows high selectivity for NO_2 gas over other gases. The inset shows high selective detection of NO_2 gas even under mixed gas flow including various gas species.

Atomic-layered MoS_2 was grown using the MoO_3 predeposited on C-plane sapphire substrate and sulfur powder.[23] Sublimated sulfur acts as a precursor to sulfurize the MoO_3 film. To achieve our overall goal of preparing MoS_2 films of consistent quality on the desired substrates, we turned our attention to pressure control during the CVD reaction. A recent report indicated that increasing Mo or S atoms enabled the formation of energetically favorable defects on MoS_2 during film growth.[15] Thus, we systematically controlled the reaction pressure to provide sufficient sublimated sulfur via a custom-made automatic pressure control system.

The uniform MoS_2 film on 2-in. sapphire substrate was synthesized, as illustrated in Figure 1a. The as-synthesized trilayered MoS_2 is semitransparent. Cross-sectional TEM was used to examine the number of layers (Figure 1b). The synthesized MoS_2 films contained mainly triple layers of 2.2 nm, which was also consistent with large-scale TEM characterization (Supporting Information, Figure S1). A planar high-resolution TEM image in Figure 1c shows a Moiré pattern typical of overlapping misoriented layers of MoS_2. We also found out that the MoS_2 film synthesized by CVD consists of polycrystalline structures, which was revealed by the diffraction pattern image obtained by fast Fourier transformation analysis (Supporting Information, Figure S2). Raman spectrum represents the in-plane vibrational mode of the Mo and S atoms (E_{2g}) and out-of-plane vibrational mode of S atoms (A_{1g}) from the as-synthesized MoS_2 film,[25] as shown in Figure 1d. The peak position difference (Δ) between E_{2g} and A_{1g} was approximately 23. It also supports that the as-synthesized MoS_2 has a trilayered film.[24,26,27] To confirm the uniform synthesis of atomic-layered MoS_2, a Raman mapping image technique was also applied to the area of 50 × 50 μm^2 at 0.3 μm laser step. The blue and red models illustrate the spatial distributions of E_{2g} and A_{1g}, respectively (Supporting Information, Figure S3).

DOI: 10.1021/am508535x
ACS Appl. Mater. Interfaces 2015, 7, 2952−2959

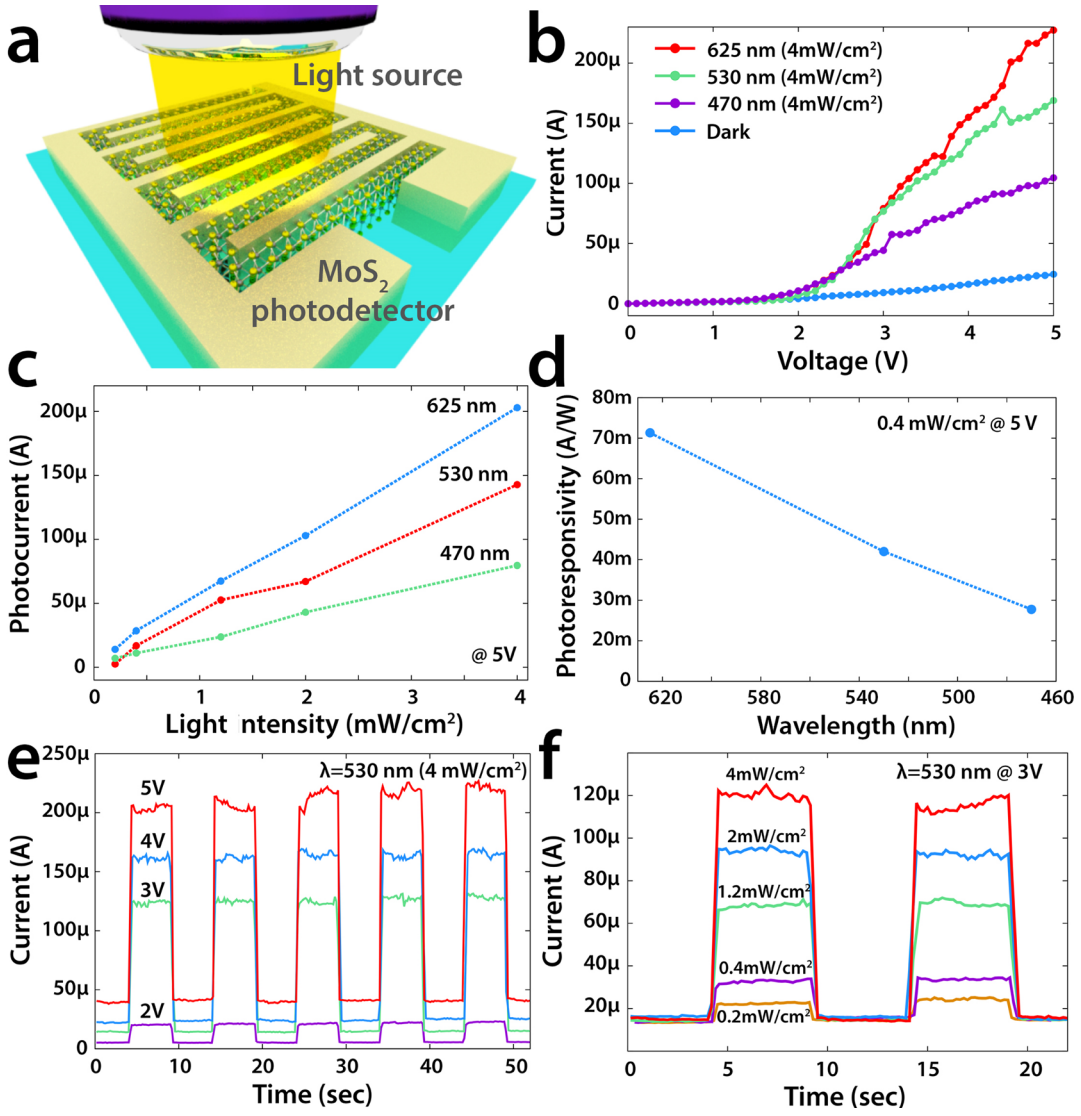

Figure 3. (a) 3D schematic image of the MoS_2 photosensing device under light illumination. (b) $I-V$ curves for the MoS_2 device in the dark and under light illumination (visible wavelengths of 625, 530, and 470 nm with an intensity of 4 mW/cm^2). The Schottky contact formed between the MoS_2 semiconducting channel and metal electrodes resulted in nonlinear $I-V$ behavior. (c) Photocurrents recorded at 5 V as a function of light intensity (0.2−4 mW/cm^2) for different wavelengths (625, 530, and 470 nm). The photocurrents were proportional to the light intensity. (d) Photoresponsivity measured at 5 V and an intensity of 0.4 mW/cm^2 as a function of wavelength (625, 530, and 470 nm). (e) Time-resolved photoresponse under 530 nm illumination with an intensity of 4 mW/cm^2 for an increasing reading voltage from 2 to 5 V. (f) Time-resolved photoresponse measured at 3 V under 530 nm illumination for light intensity from 0.2 to 4 mW/cm^2. All time-resolved photoresponse data were collected at intervals of 100 ms.

The mapping image appraises highly uniform MoS_2 film on the surface of the substrate in large scale. A strong photoluminescence (PL) spectrum of the as-grown MoS_2, excited by the 314 nm laser line at room temperature, was plotted in Figure 1e. The PL spectrum leads to two major emission peaks. Two major emission peaks featured at 1.834 eV (A exciton) and 1.976 eV (B exciton) are associated with direct band gap transition at the Brillouin zone K point.[28] Valence-band splitting by strong spin−orbit interaction gives rise to the energy difference.[28] Figure 1f shows the X-ray photoelectron spectroscopy (XPS) spectrum of MoS_2 with a doublet of Mo $3d_{5/2}$ (229.4 eV) and Mo $3d_{3/2}$ (232.5 eV) and S 2s (226.6 eV) [see Figure S4 (Supporting Information) for the additional XPS data]. These characterization data indicate that the as-synthesized grown MoS_2 has a uniform high-quality intrinsic structure on wafer-scale.

The uniform atomic-layered MoS_2 film was then implemented in gas molecule detection devices (Figure 2a). First of all, transient resistance responses to NO_2 analyte gas were investigated. Gas sensitivity was defined as $\Delta R/R_i = (R_g - R_i)/R_i$, where R_i and R_g represent the initial resistance and the resistance to analyte gas, respectively. In the NO_2 gas condition, resistance increased (positive sensitivity) (Figure 2b). The NO_2 acts as an electron acceptor, resulting in p-doping characteristics.[29] That is, NO_2 molecules capture electrons on the surface of n-type MoS_2, which causes the electron charge transfer from MoS_2 to the NO_2 molecules. It thereby leads to the resistance increase of the MoS_2 device. The MoS_2 device was highly sensitive even under the extremely low concentration of sub-ppm. The detection limit in our gas sensing test was measured to be 120 ppb; however, the detection at the lower concentration would be also available if considering the high

DOI: 10.1021/am508535x
ACS Appl. Mater. Interfaces 2015, 7, 2952−2959

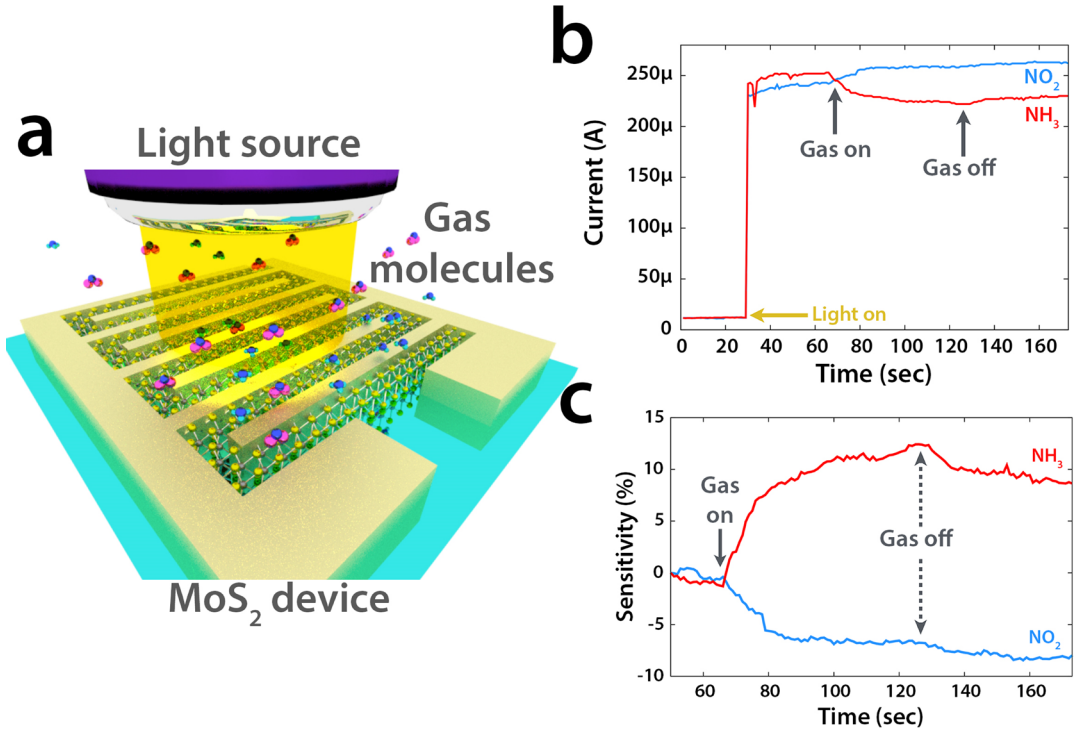

Figure 4. (a) 3D schematic image of the MoS_2 bifunctional sensing device upon exposure to gas molecules and light. (b) Sequential detection of light and gas for the MoS_2 device. The photoresponse of the MoS_2 device was detected upon 650 nm illumination with a power of 5 mW in the presence and absence of 100 ppm analyte gas (NO_2 or NH_3). Analyte gas molecules were clearly detectable even under illumination. (c) The gas sensitivities of the MoS_2 device for NO_2 and NH_3 under illumination. The data were collected at intervals of 1 s.

sensitivity of tens of percentages, even at the 120 ppb level. Especially, resistances that changed after analyte gas flow were rapidly recovered through H_2S gas flow, but it took more time to again stabilize our MoS_2 devices through N_2 flow (Supporting Information, Figure S5). The surface coverage of the adsorbed molecules for the low concentration level below 1 ppm followed the simplest isotherm model that is derived from Langmuir's theory,[30] leading to a linear relationship between sensitivity and gas concentration, as shown in Figure 2c. This suggests that charge transfer between gas molecules and sensing film dominantly contributes to the observed sensing behavior[31,32] rather than modulation of the Schottky barrier height by adsorbed molecules.[33] During the desorption process, thermal energy generally improved the desorption rate of gas molecules.[34,35] Slower adsorption to MoS_2 surface by heating to 100 °C slightly lowered the sensitivity; however, the thermal annealing could effectively increase recovery rate by accelerating the desorption process of NO_2 molecules (Figure 2d). Overall, the NO_2 sensitivity values were comparable to those of Schottky-contacted MoS_2 transistors in a recent report.[11] However, usage of the gating effect necessitates a complex peripheral circuit for a practical sensing platform. Our two-terminal structure-based gas sensor component without any gating part would be a more simple approach toward futuristic integrated sensor systems. A repetitive cycling test was also one of the important requirements for practical sensor applications. We observed that gas-sensing characteristics of our MoS_2 devices were highly stable during the cycling test upon exposure to 120 ppb of NO_2, as displayed in the left x-axis of Figure 2e. Real sensitivity values to measure peak to valley have been kept with a high sensitivity of over 50% (right y-axis of Figure 2e). To check the selectivity of MoS_2 device, sensitivities for each different gas molecule (NO_2, NH_3, H_2, and H_2S) at 100 ppm concentration were also compared, as shown in Figure 2f. Compared to the electron-donating gases, such as NH_3, H_2, and H_2S, the electron-accepting gas molecule NO_2 showed much higher sensitivity, indicating high NO_2 selectivity for our MoS_2 devices. Recent theoretical calculation, addressing adsorption energy and charge density for various molecules on MoS_2, is consistent with our experimental results.[29] The inset of Figure 2f shows that NO_2 gas could be also distinctly detectable even under mixed gas flow including 1 ppm of NO_2 and 100 ppm of NH_3 and H_2S, which would be useful for detecting specific analyte gas in a real toxic gas environment including various gas species. These highly sensitive, stable, and selective gas sensor based on 2D MoS_2 material would pave the way toward a practical sensing platform.

We now turn our focus to the investigation of photosensing characteristics under visible light illumination in ambient air utilizing atomic-layered MoS_2 (Figure 3a). Especially, in order to rule out any secondary absorption effect by light of passing through the MoS_2 film, we fabricated the device using MoS_2 transferred from semitransparent sapphire to totally opaque SiO_2/p^+ Si substrate and then performed a photosensing test. Figure 3b presents the current−voltage (I−V) curves of the MoS_2 device in the dark and under visible light (visible wavelength 625, 530, or 470 nm with a light intensity of 4 mW/cm^2). High photocurrents were generated upon exposure to the visible light sources. The Schottky contact formed between the MoS_2 semiconducting channel and the metal electrodes caused nonlinear I−V behavior.[36] The asymmetric I−V curve of the MoS_2 device also indicates that the contact interfaces between MoS_2 and Au/Cr were not precisely the same for the two terminal contact regions (Supporting Information, Figure S6). The photocurrent was proportional to the wavelength (Figure 3b). Light with a wavelength of 625 nm is most closely

DOI: 10.1021/am508535x
ACS Appl. Mater. Interfaces 2015, 7, 2952−2959

associated with the direct band gap (1.834 eV from PL) of MoS_2 and thus produced the highest photocurrent value.

The strong dependence of the photocurrent on the light intensity is illustrated in Figure 3c. The photocurrents measured at 5 V were directly proportional to the light intensity from 0.2 to 4 mW/cm^2. The photocurrent (I) versus light intensity (P) was well fitted by a power-law relationship ($I \propto P^{\alpha}$), as shown in Figure S7 (Supporting Information). The power-law exponents were calculated to be 0.84, 0.90, and 0.86 for 625, 530, and 470 nm, respectively. As the power-law exponents approach nearly 1, the amount of photons absorbed by MoS_2 itself becomes dominant for the generation rate of photocarriers, while the contribution of the defects to photocurrent generation is weak.[37,38] The photoresponsivity, a critical factor in evaluating photodetector performance, ranged from 28 to 71 mA/W under different wavelength light sources (Figure 3d), comparable to recently reported values.[39] The photosensing performance would be further increased by optimizing contact metal or device architecture. We also evaluated the transient photoresponse characteristics under voltage or intensity variation. As shown in Figure 3e, as the applied voltage increased from 2 to 5 V, the time-resolved photocurrent also increased, consistent with the $I-V$ behavior in Figure 3b. Despite some fluctuation in the saturated photocurrent (the flat region under illumination), we did not observe any serious baseline shift during the cycling test. Furthermore, we obtained good photosensing stability in the repetitive cycling test with variations in the wavelength or reading voltage [see Figure S8 (Supporting Information) for details]. The photoswitching speed of our MoS_2 photodetector was less than 500 ms, indicating that rapid band-to-band recombination of the electron−hole pairs was dominant [refer to Figure S8 (Supporting Information) for a detailed description]. Figure 3f shows the transient photoresponse under different light intensities (0.2−4 mW/cm^2). The photocurrent was proportional to the intensity of light, resulting in a stable intensity-modulated photocurrent. The excellent photosensing characteristics of our MoS_2 device, including the light- or intensity-modulated photocurrent, good photoresponsivity, and rapid transient photoresponse, will enable photonic sensing applications.

Finally, we turned our attention to the sequent detection of two environmental parameters (here, gas molecules and light source) utilizing a MoS_2-based sensing device for advanced multifunctional applications (Figure 4a). In accordance with our overall goal, we tested the gas-sensing characteristics of MoS_2 with light illumination [refer to Figure S9 (Supporting Information) for test configuration]. At the time of 30 s, large photocurrent was generated by turning on the laser source (wavelength of 650 nm with a power of 5 mW) (Figure 4b), and then the MoS_2 devices were continually exposed to the light source. Gas injection at 60 s induced relatively low gas responses compared with the photoresponse; nevertheless, analyte gas molecules were clearly detectable under illumination. Figure 4c shows the sensitivity of representative electron-accepting and -donating molecules (NO_2 and NH_3) at a gas concentration of 100 ppm under light illumination. The overall sensitivities were smaller under light illumination than those under dark (Supporting Information, Figure S10). The possible reasons of such a phenomenon are as follows: when there are so many photocarriers generated under strong illumination, not all the excited electrons/holes react with gas molecules, and thus, the portion of reacted carriers decreases.[40] Furthermore, the light-induced activation can lead to the desorption rate being faster than the adsorption rate.[40] Interestingly, atomic-layered MoS_2 transferred onto the SiO_2/p^+ Si substrate exhibited negative gas sensitivity for NO_2 (i.e., p-type behavior was observed, while MoS_2 grown on sapphire showed the n-type behavior, as shown in Figure 2b). Defect states (dangling bonds, impurities, and so on) at the semiconductor/substrate interface can redefine the effective Fermi level within gap states, modulating the conductive properties of MoS_2.[41] It was reported that the oxygen dangling bonds on a silanol-terminated SiO_2 surface can result in creating a p-type MoS_2 semiconductor.[41] The transistor V_g-I_d curves measured from the transferred MoS_2 partly support this explanation (Supporting Information, Figure S11). The significantly reduced NO_2 sensitivity on transferred MoS_2 might be also due to the conversion of major carrier type. Further studies would be necessary to elucidate the exact origin of change in the gas-sensing characteristics. Nevertheless, the demonstrated multi-sensing functionality provides the potential of atomic-layered transition-metal dichalcogenides as a new class of next-generation sensor systems.

CONCLUSION

Futuristic bifunctional sensing characteristics were demonstrated in few-layered MoS_2 based on the wafer-scale synthesis of MoS_2 via the developed CVD technique. Pressure control in the reaction chamber provided an effective sulfur source to synthesize atomic-layered MoS_2 on a large scale. We accordingly demonstrated the gas-sensing and photodetection characteristics of these synthesized MoS_2 thin films. Excellent gas sensing (extremely low detection limit of 120 ppb, high NO_2 selectivity, and stable cycling behavior) and photosensing (moderate photoresponsivity of ∼71 mA/W, reliable photoresponse, and rapid photoswitching within 500 ms) in atomic-layered 2D MoS_2 could be implemented, respectively. Finally, we have investigated the bifunctional sensing characteristics of MoS_2-based devices exposed to both gas molecules and a light source. These multifunctional sensing characteristics in atomic-layered MoS_2 make this material attractive for futuristic sensor technologies.

ASSOCIATED CONTENT

Supporting Information

Cross-sectional TEM image of as-grown MoS_2 film, planar TEM images of trasferred MoS_2 film, Raman mapping images of as-synthesized MoS_2 film, XPS analysis of MoS_2 nanofilm, comparison of the decay behavior depending on a kind of recovery gas, asymmetric $I-V$ characteristics of MoS_2 photodetector under dark or light condition, power-law relationship ($I \propto P^{\alpha}$) between photocurrent (I) and light intensity (P) of MoS_2 photodetector, photoresponse variation of MoS_2 photodetector, test setup configuration for bifunctional sensing measurement, gas sensitivity comparison of transferred MoS_2 in dark or light condition, and bottom gate MoS_2 transistor. This material is available free of charge via the Internet at http://pubs.acs.org

AUTHOR INFORMATION

Corresponding Authors

*B.C. e-mail: bjcho@kims.re.kr.
*D.-H.K. e-mail: dhkim2@kims.re.kr.
*M.G.H. e-mail: mghahm@kims.re.kr.

DOI: 10.1021/am508535x
ACS Appl. Mater. Interfaces 2015, 7, 2952−2959

Present Addresses

[§](For S.L.) Department of Chemical Engineering and Materials Science, Stevens Institute of Technology, Hoboken, NJ 07030, United States.

[∥](For C.G.K.) Cambridge Graphene Center, University of Cambridge, 9 JJ Thomson Avenue, Cambridge, United Kingdom.

Author Contributions

B.C., A.R.K., and Y.P. contributed equally to this work. B.C., D.-H.K., and M.G.H. designed and supervised the experiment. B.C., A.R.K., Y.P., and M.G.H. synthesized MoS_2 nanofilm. B.C., A.R.K., Y.P., J.Y., Y.-J.L., and M.G.H. performed the characterization of the MoS_2. B.C. and A.R.K. fabricated the MoS_2-based sensing devices. B.C., S.L., T.J.Y., and C.G.K. measured the MoS_2 sensing devices. B.C., B.H.L., H.C.K., D.-H.K., and M.G.H. analyzed the data. B.C., M.G.H., and D.-H.K cowrote the paper. All authors discussed the results and commented on the manuscript.

Notes

The authors declare no competing financial interest.

■ ACKNOWLEDGMENTS

This study was supported financially by the Fundamental Research Program (PNK3770) of the Korean Institute of Materials Science (KIMS). M.G.H. and B.C. are grateful for support from the Basic Science Research Program of the National Research Foundation of Korea (NRF) funded by the Ministry of Science, ICT & Future Planning (NRF-2014R1A1A1006214 and NRF-2014R1A1A1036139).

■ REFERENCES

(1) Franklin, A. D. Electronics: The Road to Carbon Nanotube Transistors. *Nature* **2013**, *498*, 443−444.

(2) Shulaker, M. M.; Hills, G.; Patil, N.; Wei, H.; Chen, H.-Y.; Wong, H.-S. P.; Mitra, S. Carbon Nanotube Computer. *Nature* **2013**, *501*, 526−530.

(3) Novoselov, K. S.; Fal'ko, V. I.; Colombo, L.; Gellert, P. R.; Schwab, M. G.; Kim, K. A Roadmap for Graphene. *Nature* **2012**, *490*, 192−200.

(4) Ganatra, R.; Zhang, Q. Few-Layer MoS_2: A Promising Layered Semiconductor. *ACS Nano* **2014**, *8*, 4074−4099.

(5) Sun, Z.; Chang, H. Graphene and Graphene-like Two-Dimensional Materials in Photodetection: Mechanisms and Methodology. *ACS Nano* **2014**, *8*, 4133−4156.

(6) Jariwala, D.; Sangwan, V. K.; Lauhon, L. J.; Marks, T. J.; Hersam, M. C. Emerging Device Applications for Semiconducting Two-Dimensional Transition Metal Dichalcogenides. *ACS Nano* **2014**, *8*, 1102−1120.

(7) Yang, S.; Li, Y.; Wang, X.; Huo, N.; Xia, J.-B.; Li, S.-S.; Li, J. High Performance Few-Layer GaS Photodetector and Its Unique Photo-Response in Different Gas Environments. *Nanoscale* **2014**, *6*, 2582−2587.

(8) Yang, S.; Tongay, S.; Yue, Q.; Li, Y.; Li, B.; Lu, F. High-Performance Few-Layer Mo-Doped $ReSe_2$ Nanosheet Photodetectors. *Sci. Rep.* **2014**, *4*, 5442.

(9) Perkins, F. K.; Friedman, a L.; Cobas, E.; Campbell, P. M.; Jernigan, G. G.; Jonker, B. T. Chemical Vapor Sensing with Monolayer MoS_2. *Nano Lett.* **2013**, *13*, 668−673.

(10) Yao, Y.; Tolentino, L.; Yang, Z.; Song, X.; Zhang, W.; Chen, Y.; Wong, C. High-Concentration Aqueous Dispersions of MoS_2. *Adv. Funct. Mater.* **2013**, *23*, 3577−3583.

(11) He, Q.; Zeng, Z.; Yin, Z.; Li, H.; Wu, S.; Huang, X.; Zhang, H. Fabrication of Flexible MoS_2 Thin-Film Transistor Arrays for Practical Gas-Sensing Applications. *Small* **2012**, *8*, 2994−2999.

(12) Li, H.; Yin, Z.; He, Q.; Li, H.; Huang, X.; Lu, G.; Fam, D. W. H.; Tok, A. I. Y.; Zhang, Q.; Zhang, H. Fabrication of Single- and Multilayer MoS_2 Film-Based Field-Effect Transistors for Sensing NO at Room Temperature. *Small* **2012**, *8*, 63−67.

(13) Lopez-Sanchez, O.; Lembke, D.; Kayci, M.; Radenovic, A.; Kis, A. Ultrasensitive Photodetectors Based on Monolayer MoS_2. *Nat. Nanotechnol.* **2013**, *8*, 497−501.

(14) Roy, K.; Padmanabhan, M.; Goswami, S.; Sai, T. P.; Ramalingam, G.; Raghavan, S.; Ghosh, A. Graphene−MoS_2 Hybrid Structures for Multifunctional Photoresponsive Memory Devices. *Nat. Nanotechnol.* **2013**, *8*, 826−830.

(15) Najmaei, S.; Liu, Z.; Zhou, W.; Zou, X.; Shi, G.; Lei, S.; Yakobson, B. I.; Idrobo, J.-C.; Ajayan, P. M.; Lou, J. Vapour Phase Growth and Grain Boundary Structure of Molybdenum Disulphide Atomic Layers. *Nat. Mater.* **2013**, *12*, 754−759.

(16) Zheng, J.; Zhang, H.; Dong, S.; Liu, Y.; Nai, C. T.; Shin, H. S.; Jeong, H. Y.; Liu, B.; Loh, K. P. High Yield Exfoliation of Two-Dimensional Chalcogenides Using Sodium Naphthalenide. *Nat. Commun.* **2014**, *5*, 2995.

(17) Song, I.; Park, C.; Hong, M.; Baik, J.; Shin, H.-J.; Choi, H. C. Patternable Large-Scale Molybdenium Disulfide Atomic Layers Grown by Gold-Assisted Chemical Vapor Deposition. *Angew. Chem., Int. Ed.* **2014**, *53*, 1266−1269.

(18) Ling, X.; Lee, Y.-H.; Lin, Y.; Fang, W.; Yu, L.; Dresselhaus, M. S.; Kong, J. Role of the Seeding Promoter in MoS_2 Growth by Chemical Vapor Deposition. *Nano Lett.* **2014**, *14*, 464−472.

(19) Li, B.; Yang, S.; Huo, N.; Li, Y.; Yang, J.; Li, R.; Fan, C.; Lu, F. Growth of Large Area Few-Layer or Monolayer MoS_2 from Controllable MoO_3 Nanowire Nuclei. *RSC Adv.* **2014**, *4*, 26407−26412.

(20) Yang, H.; Heo, J.; Park, S.; Song, H. J.; Seo, D. H.; Byun, K.-E.; Kim, P.; Yoo, I.; Chung, H.-J.; Kim, K. Graphene Barristor, a Triode Device with a Gate-Controlled Schottky Barrier. *Science* **2012**, *336*, 1140−1143.

(21) Cunningham, G.; Khan, U.; Backes, C.; Hanlon, D.; McCloskey, D.; Donegan, J. F.; Coleman, J. N. Photoconductivity of Solution-Processed MoS_2 Films. *J. Mater. Chem. C* **2013**, *1*, 6899−6904.

(22) Lee, Y.; Lee, J.; Bark, H.; Oh, I.-K.; Ryu, G. H.; Lee, Z.; Kim, H.; Cho, J. H.; Ahn, J.-H.; Lee, C. Synthesis of Wafer-Scale Uniform Molybdenum Disulfide Films with Control over the Layer Number Using a Gas Phase Sulfur Precursor. *Nanoscale* **2014**, *6*, 2821−2826.

(23) Lin, Y.-C.; Zhang, W.; Huang, J.-K.; Liu, K.-K.; Lee, Y.-H.; Liang, C.-T.; Chu, C.-W.; Li, L.-J. Wafer-Scale MoS_2 Thin Layers Prepared by MoO_3 Sulfurization. *Nanoscale* **2012**, *4*, 6637−6641.

(24) Liu, K.-K.; Zhang, W.; Lee, Y.-H.; Lin, Y.-C.; Chang, M.-T.; Su, C.-Y.; Chang, C.-S.; Li, H.; Shi, Y.; Zhang, H.; et al. Growth of Large-Area and Highly Crystalline MoS_2 Thin Layers on Insulating Substrates. *Nano Lett.* **2012**, *12*, 1538−1544.

(25) Bertrand, P. A. Surface-Phonon Dispersion of MoS_2. *Phys. Rev. B* **1991**, *44*, 5745−5749.

(26) Li, S.; Miyazaki, H.; Song, H.; Kuramochi, H.; Nakaharai, S.; Tsukagoshi, K. Quantitative Raman Spectrum and Reliable Thickness Identification for Atomic Layers on Insulating Substrates. *ACS Nano* **2012**, *6*, 7381−7388.

(27) Liu, Y.; Nan, H.; Wu, X.; Pan, W.; Wang, W.; Bai, J.; Zhao, W.; Sun, L.; Wang, X.; Ni, Z. Layer-by-Layer Thinning of MoS_2 by Plasma. *ACS Nano* **2013**, *7*, 4202−4209.

(28) Mak, K. F.; Lee, C.; Hone, J.; Shan, J.; Heinz, T. F. Atomically Thin MoS_2: A New Direct-Gap Semiconductor. *Phys. Rev. Lett.* **2010**, *105*, 136805.

(29) Yue, Q.; Shao, Z.; Chang, S.; Li, J. Adsorption of Gas Molecules on Monolayer MoS_2 and Effect of Applied Electric Field. *Nanoscale Res. Lett.* **2013**, *8*, 425.

(30) Laidler, K. J. *Chemical Kinetics*; McGraw-Hill Book Co.: New York, 1965.

(31) Abbas, A. N.; Liu, G.; Liu, B.; Zhang, L.; Liu, H.; Ohlberg, D.; Wu, W.; Zhou, C.; Engineering, E.; California, S.; et al. Chemical Sensing Applications of Graphene Nanoribbon Arrays Down to 5 Nm Using Helium Ion Beam. *ACS Nano* **2014**, *8*, 1538−1546.

DOI: 10.1021/am508535x
ACS Appl. Mater. Interfaces 2015, 7, 2952−2959

(32) Zhang, D.; Liu, Z.; Li, C.; Tang, T.; Liu, X.; Han, S.; Lei, B. Detection of NO_2 down to Ppb Levels Using Individual and Multiple In_2O_3 Nanowire Devices. *Nano Lett.* **2004**, *4*, 1919−1924.
(33) Liu, B.; Chen, L.; Liu, G.; Abbas, A. N.; Fathi, M.; Zhou, C. High-Performance Chemical Sensing Using Schottky-Contacted Chemical Vapor Deposition Grown Monolayer MoS_2 Transistors. *ACS Nano* **2014**, *8*, 5304−5314.
(34) Yavari, F.; Chen, Z.; Thomas, A. V.; Ren, W.; Cheng, H.-M.; Koratkar, N. High Sensitivity Gas Detection Using a Macroscopic Three-Dimensional Graphene Foam Network. *Sci. Rep.* **2011**, *1*, 166.
(35) Choi, H.; Choi, J. S.; Kim, J.-S.; Choe, J.-H.; Chung, K. H.; Shin, J.-W.; Kim, J. T.; Youn, D.-H.; Kim, K.-C.; Lee, J.-I.; et al. Flexible and Transparent Gas Molecule Sensor Integrated with Sensing and Heating Graphene Layers. *Small* **2014**, *10*, 3812.
(36) Liou, L. C.; Nabet, B. Simple Analytical Model of Bias Dependence of the Photocurrent of Metal−Semiconductor−Metal Photodetectors. *Appl. Opt.* **1996**, *35*, 15−23.
(37) Xia, F.; Mueller, T.; Lin, Y.-M.; Valdes-Garcia, A.; Avouris, P. Ultrafast Graphene Photodetector. *Nat. Nanotechnol.* **2009**, *4*, 839−843.
(38) Mueller, T.; Xia, F.; Avouris, P. Graphene Photodetectors for High-Speed Optical Communications. *Nat. Photonics* **2010**, *4*, 297−301.
(39) Lu, J.; Lu, J. H.; Liu, H.; Liu, B.; Chan, K. X.; Lin, J.; Chen, W.; Loh, K. P.; Sow, C. H. Improved Photoelectrical Properties of MoS_2 Films after Laser Micromachining. *ACS Nano* **2014**, *8*, 6334−6343.
(40) Late, D. J.; Huang, Y.; Liu, B.; Acharya, J.; Shirodkar, S. N.; Luo, J. Sensing Behavior of Atomically Thin-Layered MoS_2 Transistors. *ACS Nano* **2013**, *7*, 4879−4891.
(41) Dolui, K.; Rungger, I.; Sanvito, S. Origin of the n-Type and p-Type Conductivity of MoS_2 Monolayers on a SiO_2 Substrate. *Phys. Rev. B* **2013**, *87*, 165402.

DOI: 10.1021/am508535x
ACS Appl. Mater. Interfaces 2015, 7, 2952−2959